Why moist dynamic processes matter for the sub-seasonal prediction of atmospheric blocking over Europe

Jan Wandel[1,2], Dominik Büeler[1,3], Peter Knippertz[1], Julian F. Quinting[1], Christian M. Grams[1]

[1]Department of Tropospheric Research, Institute of Meteorology and Climate Research (IMK), Karlsruhe Institute of Technology (KIT), Karlsruhe, Germany
[2]now at: Deutscher Wetterdienst, Offenbach, Germany.
[3]now at: Institute for Atmospheric and Climate Science, ETH Zurich, Switzerland.

Key Points:

- Sub-seasonal forecasts underestimate warm conveyor belt (WCB) activity around the onset of atmospheric blocking over Europe (EuBL)
- Improving WCB prediction is important to further exploit windows of opportunity of sub-seasonal EuBL forecasts
- Synoptic activity over the North Pacific supports the development of a teleconnection that is vital for EuBL onset

Corresponding author: Jan Wandel, `Jan.Wandel@dwd.de`

Abstract

Numerical weather prediction (NWP) and climate models still struggle to correctly predict and represent atmospheric blocking over the European region (EuBL). In recent years, there has been growing evidence that latent heat release in midlatitude weather systems such as warm conveyor belts (WCBs) contribute significantly to the onset and maintenance of blocking anticyclones. In this study, we show that for the European Centre for Medium-Range Weather Forecast's IFS reforecasts in extended winter (1997–2017) WCB activity around EuBL onsets becomes challenging to predict in pentad 3 (10–14 days) and beyond. This is in line with the short overall WCB forecast skill horizon of around 10 days and partly explains low EuBL skill in NWP models. However, we also show cases in which accurate WCB and EuBL forecasts are possible even in pentad 4 (15–19 days). These cases are associated with accurate WCB forecasts over the North Atlantic and North Pacific pointing towards a teleconnection between the two. Lastly, we find that WCB activity over the North Atlantic emerges way before the block is established and different pathways into EuBL exist in the reforecasts which are characterised by a westward shift of the main WCB inflow and outflow region compared to reanalysis. We conclude that despite intrinsic limits of predictability there is room to improve forecasts of EuBL onset by improving the representation of WCB activity in NWP models.

Plain Language Summary

Numerical weather prediction (NWP) and climate models have difficulties to correctly predict and represent atmospheric blocking over the European region (EuBL). In recent years, many studies find that latent heat release in midlatitude weather systems such as warm conveyor belts (WCBs) have a strong impact on the development and maintenance of EuBL. In this study, we show that for the NWP model from the European Centre for Medium-Range Weather Forecast (1997–2017) WCB activity around EuBL onsets is difficult to predict 10–14 days in the future and beyond. This is in line with the ability of the NWP model to predict WCBs and partly explains the challenges in EuBL prediction. However, we also show cases in which accurate WCB and EuBL forecasts are possible even 15–19 days in the future. These cases are associated with good WCB forecasts over the North Atlantic and North Pacific. Lastly, we find that different pathways into EuBL exist in the forecasts which are characterised by a westward shift of the main WCB region compared to observations. We conclude that there is room to improve forecasts of EuBL onset by improving the representation of WCB activity in NWP models.

1 Introduction

Atmospheric blocking describes the formation of persistent, large-scale anticyclonic circulation anomalies that block the westerly flow and eastward propagation of synoptic eddies (Berggren et al., 1949; Rex, 1950). Blocking can be associated with extreme weather events such as heat waves or thunderstorm episodes in summer (Pfahl & Wernli, 2012; Mohr et al., 2019) and cold spells in winter (Buehler et al., 2011; Ferranti et al., 2018). Thus, the accurate prediction of blocking on sub-seasonal to seasonal (S2S) time scales is desirable for decision makers to prepare for extreme weather events and to issue early warnings. Early blocking studies developed theories for the formation and maintenance of blocking by planetary waves or orographic forcing (Charney & DeVore, 1979; Hoskins & Karoly, 1981). However, they could not explain some observed characteristics such as the rapid onset (Nakamura & Huang, 2018) or the fluctuation in size and intensity during the blocking life cycle (Dole, 1986).

These restrictions point to the importance of transient eddies and synoptic-scale processes for the formation and maintenance of atmospheric blocking (Shutts, 1983). Until recently, the evaluation of these processes has almost exclusively been done on the basis of dry dynamics (Colucci, 1985; Yamazaki & Itoh, 2013). However, moist dynamic processes, in particular latent heat release (LHR) due to cloud formation, are a first-order process for the onset and maintenance of atmospheric blocking (Pfahl et al., 2015). LHR plays an important role in modifying the large-scale flow through cross-isentropic ascent and divergent outflow in the upper troposphere (Pomroy & Thorpe, 2000; Grams et al., 2011). Intense LHR occurs in poleward ascending air streams in the warm sector of extratropical cyclones, in so-called warm conveyor belts (WCBs) (Wernli, 1997; Madonna et al., 2014). It is the diabatically enhanced outflow of these rapidly ascending air streams that contributes considerably to the onset (rapid amplification of synoptic ridges) and maintenance of persistent blocks (Steinfeld & Pfahl, 2019). WCBs are challenging to predict due to the small-scale processes associated with the air streams. Skillful predictions of WCBs in current numerical weather prediction (NWP) models are possible until around 8–10 days (Wandel et al., 2021).

The representation of atmospheric blocking in NWP and climate models has been investigated in numerous studies in the last two decades. Many studies point to the underestimation of blocking frequency (negative bias) over the European region (d'Andrea et al., 1998; Masato et al., 2014). This bias increases with longer lead time (Jia et al., 2014; Quinting & Vitart, 2019) and can be reduced with higher horizontal and vertical resolution (Dawson et al., 2012; Anstey et al., 2013; Davini et al., 2017). Remarkably, the year-round forecast horizon for blocking over the Central European region is 3–5 days shorter compared to other large-scale flow regimes (Büeler et al., 2021). NWP models particularly struggle predicting the onset of EuBL (Rodwell et al., 2013; Ferranti et al., 2015). These difficulties can partly be linked to its lower intrinsic predictability (Faranda et al., 2016; Hochman et al., 2021), but might also be a result of physical processes, such as LHR in WCBs, which are still difficult for the models to accurately capture.

In a recent study Grams et al. (2018) highlight the role of WCBs for the onset of blocking over Europe in one of the most severe forecast busts in the ECMWF's integrated forecasting system (IFS) in the last decade. They find that a misrepresentation of the WCB in the ensemble forecasting system amplified the initial condition error and triggered a nonlinear feedback mechanism. The WCB communicated the forecast error from small scales to the upper troposphere and downstream that led to the missed onset of the block. Other studies also point to the amplification of errors in the WCBs (Pickl et al., 2023) or highlight the generation of errors in potential temperature and potential vorticity in the WCBs, which can lead to downstream errors in the Rossby wave pattern (Martínez-Alvarado et al., 2016; Berman & Torn, 2019). Moreover, teleconnections from the Caribbean and North Pacific region affect the occurrence of large-scale weather regimes, including blocking, in the European region (Michel & Rivière, 2011; Michel et al., 2012; Quinting et al., 2023). In summary, these studies suggest that a more accurate representation of WCB anomalies may reduce forecast uncertainty in the downstream wave guide leading to a better prediction of atmospheric blocking over Europe. However, a systematic investigation of the role of WCBs for the prediction of atmospheric blocking over Europe is still missing.

Here, we evaluate the systematic link between WCBs and blocking, by addressing the following three research questions and using ECMWF's IFS S2S reforecasts and reanalysis in the extended winter period from 1997–2017.

- What is the link between WCB activity and EuBL onset and how well is it represented in reforecasts at different forecast lead times?
- Is there a link between WCB representation and correct forecasts of EuBL onset?
- Do teleconnections from the North Pacific region play a role for the prediction of EuBL?

We focus on EuBL onsets in different pentads (lead times of 0–4 days, 5–9 days, 10–14 days, and 15–19 days) since forecast skill for Atlantic-European weather regimes and WCBs on average vanishes in week 2 (7-14 days) (Büeler et al., 2021; Wandel et al., 2021; Osman et al., 2023). Onsets of large-scale and persistent flow regimes at lead times of 5–20 days are of particular interest from a sub-seasonal prediction perspective, because, due to their persistence, they strongly influence the circulation even beyond lead times of 20 days.

The data, the definition of EuBL, and the Eulerian metric to identify WCBs are introduced in section 2. Section 3 investigates the role of WCBs for atmospheric blocking over Europe and its representation in the reforecasts across different forecast lead times. Section 4 then explores potential causalities between WCB activity and the forecast of EuBL. The role of upstream precursors from the Pacific for the prediction of EuBL is further analysed in section 5 and the study ends with concluding remarks in section 6.

2 Data and Method

2.1 Reforecasts and reanalysis

We use the ECMWF's IFS sub-seasonal ensemble reforecasts (Vitart, 2017) for the extended winter period (NDJFM) from 1997–2017 to analyze WCBs and 500-hPa geopotential height (Z500). The ensemble reforecasts contain in total 11 members, of which one member is an unperturbed control forecast. To increase our sample size we use all reforecasts for IFS cycles CY43R1, CY43R3, and CY45R1, yielding a total of 1641 initialisation times. Consistently with the initial conditions of the reforecasts, we employ ERA-Interim reanalysis data (Dee et al., 2011) for verification. Both data sets are retrieved on a regular 1.5×1.5 latitude–longitude grid and remapped to 1×1 grid spacing. We calibrate the reforecasts by calculating WCB and Z500 anomalies relative to the 90-day running mean model climatology at a given lead time derived from the 20-year reforecast data using all cycles. Anomalies for ERA-Interim are computed against ERA-Interim climatology for 1997–2017. This approach eliminates the systematic bias between ERA-Interim and the reforecasts.

2.2 Atlantic-European weather regimes

To identify blocking over the European region, we use seven year-round Atlantic-European weather regimes based on 5-day low-pass-filtered geopotential height (Grams et al., 2017; Büeler et al., 2021). Thus, we refer to atmospheric blocking using the definition of blocked weather regimes. Weather regimes are quasi-stationary, persistent, and recurrent large-scale flow patterns in the midlatitudes (Vautard, 1990; Michelangeli et al., 1995) and reflect the variability of the large-scale extratropical circulation on sub-seasonal timescales. An accurate prediction of large-scale flow regimes is particularly important since it yields more information about different surface variables (e.g. temperature and precipitation) after forecast day 10–15 compared to the direct NWP model output (Bloomfield et al., 2021; Mastrantonas et al., 2022). Blocking over the European region (EuBL) is the dominant blocked regime in winter (compared to "Scandinavian Blocking" in summer) and occurs at around 11% of winter days. For the computation of the regime patterns the interested reader is referred to Büeler et al. (2021).

2.3 Warm conveyor belts

The stages of WCB inflow, ascent, and outflow are identified using a novel framework of convolutional neural networks (CNNs) introduced by Quinting and Grams (2022). The CNN-based metric (ELIAS2.0) is designed to evaluate WCBs in large data sets at low spatio-temporal resolution for which the original trajectory-based WCB definition (Wernli & Davies, 1997) is not applicable. The method now facilitates for the first time a systematic study of WCBs in a large data set. It takes meteorological parameters as predictors, which are characteristic of each WCB stage, and predict two-dimensional WCB footprints. The CNN method successfully reproduces the climatological distribution of WCBs found with the trajectory-based approach (Madonna et al., 2014) and skillfully identifies WCBs at instantaneous time steps.

2.4 EuBL in reanalysis and reforecasts

2.4.1 Forecast perspective and lead times

In our study, we focus on EuBL events in the extended winter period from 1997–2017. Following Grams et al. (2017) and Büeler et al. (2021), an EuBL onset is identified at the first time when the respective weather regime index I_{wr} exceeds a threshold of 0.9 and remains above this threshold for at least five consecutive days. Here, we refer to onset in a given pentad, if the onset date lays within that pentad (see schematic in Fig. 1). In order to directly compare ERA-Interim to the reforecasts, we treat ERA-Interim as a "perfect ensemble member" for each respective forecast and identify EuBL onset and life cycles in the same manner as for individual ensemble members. Therefore, we match ERA-Interim to each available reforecast initialisation time and lead time. In total, there are 38 EuBL events in ERA-Interim in the period from 1997–2017. When investigated from a forecast perspective, this number increases because each individual event is captured multiple times by different forecasts. For example, ERA-Interim onsets of EuBL that occur in pentad 3 of the forecast (10–14 days lead time) are captured on average by 2.6 forecasts, which increases the number of events from 38 to 98 (Table 1). Since the reforecasts are not available on a daily basis, this approach weights the ERA-Interim events according to the available initialisation times of the reforecasts and allows for a direct comparison to the events in the reforecasts. While the reforecasts are evaluated in pentad 2 (forecast day 5–9), pentad 3 (day 10–14) and pentad 4 (day 15–19), fields in ERA-Interim are only shown for EuBL onsets in pentad 3, which is the main focus of the study. At the same time the perfect member forecast by ERA-Interim for onsets in pentad 2 or 4 hardly differs from the one evaluated in pentad 3, as the underlying data is almost similar, except for the slightly different samples due to the incomplete availability of reforecast initialisation times (not shown). Onsets in pentad 3 are of particular interest since both, the regime and WCB skill, vanish around the 8–10 day lead time.

2.4.2 Different approaches to link WCBs and EuBL

To assess the role of WCBs for the onset of EuBL, we analyse Z500 and the WCB activity using two different approaches: first, for each pentad we calculate 5-day mean composites around ERA-Interim onsets to understand characteristics of EuBL in reanalyses and to evaluate the representation of the patterns in the reforecasts at different forecast lead times. We focus on pentads for fixed lead times rather than centred composites around the actual onset date to avoid biases due to mixing different forecast lead times. Second, we investigate the six days prior to onset using lagged composites which are stratified on individual onset dates in reanalysis and reforecasts. This approach allows a direct comparison of the evolution of the fields while giving hints to potential causalities between WCBs and the blocked regime.

Furthermore, we distinguish between the ensemble mean of the reforecasts and individual ensemble members which are selected depending on their forecast performance. On the one hand, the ensemble mean of the reforecasts is used to evaluate their ability in representing ERA-Interim EuBL onsets across different lead times. On the other hand, individual ensemble members from different initialisation times are grouped together, depending on their ability to represent EuBL to explore potential deficiencies in the model related to the link of WCB activity and blocking onset. Ensemble members that correctly (within two days) capture an ERA-Interim EuBL onset are defined as "Hits", members which do not capture the onset as "Misses". Furthermore, we include all ensemble members in our analysis that predict an EuBL onset while no event is analysed in ERA-Interim ("False Alarms").

As stated above, we find 38 unique EuBL events in ERA-Interim during either pentads 2, 3, or 4 of the available reforecasts initialised in the 20 year period 1997–2017. These could in principle be captured by 98 forecast initialisation times. Thus, 98 x 11 = 1078 individual forecasts by one of the ensemble members that could either identify (Hit) or not identify (Miss) these EuBL onsets. In addition forecasts can issue a false alarm.

For 34 out of the 38 unique ERA-Interim events, there is at least one ensemble member that correctly captures the EuBL onset (Hit) for onsets in pentad 2 (4 unique events are completely missed) (Table 1). This number of captured unique events decreases for onsets in pentad 3 and 4 (29 and 26 unique events, respectively). Each unique EuBL event is captured by more than one forecast since the reforecasts are initialised multiple times per week (see "forecast perspective" with 72/45/34 Hits for EuBL onsets in pentad 2/3/4). When the EuBL is captured by these forecasts, mostly 1–2 ensemble members correctly predict the onset in pentad 2. There are also events that are captured by 3–11 ensemble members, which results in a total of 271 ensemble members (25 % of all possible ensemble members) capturing a EuBL onset in pentad 2. For onsets in pentad 3 this number decreases to 65 (6 %) with the events being mostly captured by 1–2 ensemble members and some by 3–4. In pentad 4, there are 41 ensemble members (3 % of all possible ensemble members) that capture the 26 unique EuBL events. The analysis shows that the accurate representation of EuBL becomes more challenging with forecast lead time. Still, in pentad 4, 26 out of the 38 unique events are captured by at least one ensemble member, which provides robustness to our further analysis.

The Misses category contains all ensemble members which do not capture the onset of the observed EuBL event. Naturally, this number is highest for onsets in pentad 4 when the number of Hits is lowest. It is important to note that ensemble members in the Misses category can theoretically project in any other large-scale flow regime. Lastly, the ensemble members which predict a EuBL onset but without a corresponding observed EuBL onset in ERA-Interim make up the False Alarms category. Out of the 1641 forecast initialisation times in the reforecast period, there are 362 with at least one ensemble members with a False Alarm in pentad 2. The number of False Alarms is even higher in pentad 3 and 4.

3 The role of WCBs for EuBL prediction

We first investigate the spatial patterns of Z500, as well as WCB inflow and outflow occurrence frequencies around EuBL onsets in ERA-Interim in pentad 3 (10–14 days, Fig. 2). The 5-day mean ERA-Interim Z500 field shows marked positive Z500 anomalies of 90–110 gpm extending from western Europe to Scandinavia (Fig. 2c). These anomalies reflect the developing block over Europe. Upstream, negative anomalies (–70 to – 90 gpm) indicate a trough over the western and central North Atlantic. The strong positive and negative Z500 anomalies are in line with the climatological pattern of the EuBL regime (green contours in Fig. 2, see Grams et al. (2017)). The large-scale circulation over North America and the North Pacific indicates a weakly undulated jet stream (dense isohypses, black in Fig. 2c) with anomalous Rossby wave packets along the midlatitude jet (reflected in pairs of negative Z500 anomalies over the western part of the North Pacific/western North America and positive Z500 anomalies over the eastern North Pacific/East coast of North America). The anomalous Rossby wave activity might be an important precursor of EuBL events and important for its predictability. We further discuss upstream precursors in Section 5.

Enhanced WCB inflow occurs during the EuBL onset in a region stretching from south of Newfoundland into the central North Atlantic (5-day mean anomalies of 4–8%; Fig. 2a). The strongest WCB inflow anomalies can be found on the southern side of the upper level trough. The air masses typically converge in the WCB inflow region and are subsequently lifted to the mid and upper troposphere due to strong vertical lifting in the vicinity of surface cyclones. The air masses then reach the upper troposphere further to the northeast of the inflow region. Consequently, around EuBL onsets, enhanced WCB outflow frequencies occur northeast of the inflow region in an area around Iceland and over the Norwegian Sea (Fig. 2b). Here, the 5-day mean outflow frequency anomalies reach 4–6% - more than double the climatological frequency in that region. The air masses likely influence the upper-level ridge building, which subsequently leads to the onset and persistence of the block over Europe. In summary, the characteristics of the large-scale circulation and the WCB activity around EuBL onsets corroborate that WCBs might play a vital role in the formation of the blocked regime over Europe (Pfahl et al., 2015; Steinfeld & Pfahl, 2019).

Next, we evaluate the overall forecast skill of ECMWF's IFS reforecasts in predicting WCBs. The calculation of the skill allows for an estimation of the time scales on which we expect the reforecast to correctly reproduce the WCB anomalies around EuBL onsets. As for a previous version of the Eulerian WCB metric based on logistic regression (Wandel et al., 2021), we here discuss the Fair Brier Skill Score (FBSS) (Ferro, 2014) for WCB outflow frequencies based on the CNN-based WCB metric ELIAS2.0 (Quinting & Grams, 2022). Results are shown for the entire Northern Hemisphere, as well as for sub-regions over the North Pacific and North Atlantic (see Wandel et al. (2021) for more information). In general, the reforecasts have high skill in predicting WCBs in the first days of the forecast (Fig. 3). However, the skill deteriorates relatively quickly between forecast day 5 and 9 (pentad 2) and drops below a subjective threshold of 0.08 at forecast day 8 (see Wandel et al. (2021) for explanation). In pentad 3, the reforecasts are only slightly better than a climatological reference forecasts (FBBS of around 0.05) and the skill fully vanishes at forecast day 15. This analysis shows that the WCB forecast skill vanishes at medium-range forecast lead times in forecast week 2 (between day 8–14) with large differences in WCB skill between pentad 2 (day 5–9) and 3 (day 10–14). Therefore, we focus here on pentads rather than weeks.

In the following, we evaluate how well the reforecasts can predict the large-scale circulation (in terms of Z500) and WCBs around observed EuBL onsets. In order to understand if there is a correlation between the vanishing WCB skill and the prediction of Z500 patterns, we focus on EuBL onsets in pentad 2, 3, and 4 (Fig. 4). For observed EuBL onsets in pentad 2, the ensemble mean of the reforecast correctly captures the location of the trough over the North Atlantic and the developing block over Europe (cf. Fig. 2c, Fig. 4c). Compared to ERA-Interim, the amplitude of the 5-day mean circulation anomalies is underestimated by the reforecasts by 20–40 gpm, which, however, is expected considering that we look at the ensemble mean. Over the North Pacific and North America, the anomalous Rossby wave activity is well represented.

Around observed EuBL onsets in pentad 2, the WCB inflow frequencies in the ensemble mean of the reforecasts are highest over the western North Atlantic (anomalies 1-3 %)(Fig. 4a). The main WCB inflow region is shifted westwards compared to ERA-Interim, where the highest frequencies can be found over the central North Atlantic (Fig. 2a). The main outflow region in the ensemble mean of the reforecasts is centered over the southern tip of Greenland and Iceland (Fig. 4b). The reforecasts capture the enhanced WCB outflow activity around EuBL onsets but underestimate the amplitude of the anomalies by around 3 % and somewhat exhibit a westward displacement towards Greenland (cf. Fig. 4b, Fig. 2b). Recalling the underestimation of the amplitude of the Z500 anomalies (Fig. 4c), these results indicate that there might be a link to the underestimation of WCB activity. Over the North Pacific region, WCB frequencies are strongly enhanced in the reforecasts and generally well predicted with only small underestimations compared to ERA-Interim (cf. Fig. 4a,b, Fig. 2a,b). The analysis shows that for EuBL onsets in pentad 2, the ensemble mean of the reforecast can predict the development of the block generally well together with a good prediction of WCB frequencies. However, frequency underestimations over Greenland and Iceland in the WCB outflow and a westward shift in the main WCB inflow regions hint that the WCB could contribute to the slight underestimation of Z500 anomalies.

Compared to onsets in pentad 2, regime onsets in pentad 3 are naturally more challenging for the ensemble mean of the reforecast to capture. The predicted Z500 anomalies over the North Atlantic are almost half of those in pentad 2 (Fig. 4c,f). Further upstream, the prediction of circulation anomalies over the North Pacific and North America are more similar albeit slightly weaker. Hence, the ensemble mean of reforecasts can still capture the large-scale circulation over the North Pacific and North America for observed onsets in pentad 3 but strongly underestimates the circulation anomalies over the North Atlantic. Besides the strong underestimation of Z500 anomalies, we find relatively weak WCB inflow and outflow frequency anomalies around 1.5 %(Fig. 4d,e), which are significantly lower than WCB frequencies around EuBL onsets in ERA-Interim (Fig. 2a,b). These findings are in line with the low WCB forecast skill in pentad 3 (Fig. 3) underlining the increasing challenges in predicting WCBs on these forecast lead times. The results further indicate that an accurate forecast of Z500 patterns might be limited due to the important contribution of WCB air masses and its overall low forecast skill.

Lastly, observed onsets in pentad 4 show further challenges for the ensemble mean of the reforecasts (Fig. 4i). The reforecasts predict a pattern with positive Z500 anomalies centered over the southern part of Greenland and weaker anomalies over Europe. This pattern resembles the negative phase of the North Atlantic Oscillation (NAO) rather than blocking over Europe. As for onsets in pentad 2 and 3, Z500 anomalies over the North Pacific/North America region are predicted well by the ensemble mean, which indicates the general ability of the model in predicting flow patterns on these lead times. The prediction of WCB inflow and outflow anomalies for observed onsets in pentad 4 is difficult for the ensemble mean, since WCB predictions have generally no forecast skill in pentad 4. Consequently, the ensemble mean pattern resembles the climatological distribution over the North Atlantic (Fig. 4g,h). In summary, the predictions and verifying reanalyis of WCB and Z500 anomalies over the North Atlantic and Europe around EuBL onsets suggest a potential link, which goes beyond the pure correlation and that this link is weaker beyond lead times of 10 days.

4 The importance of accurate WCB prediction

4.1 Windows of opportunity

We now further investigate the potential link between WCB activity and the correct EuBL representation in IFS reforecasts. Therefore, as described in Section 2.4, we divide the ensemble into individual ensemble members depending on their forecast performance. The ensemble members that correctly predict an observed EuBL onset ("Hits") are then compared with the members that miss an observed onset ("Misses"). Furthermore, we evaluate all ensemble members that predict an EuBL onset when the onset does not verify in ERA-Interim ("False Alarms"). The number of ensemble members in the different categories varies between the considered EuBL onsets in pentad 2, 3, and 4 (Table 1 and discussion in Section 2.4).

In pentad 4, the bulk of ensemble members (1037 of 1078) miss EuBL and only 41 ensemble members correctly predict an EuBL onset. Consequently, the ensemble mean is dominated by theses misses and shows no anomalous WCB activity and a NAO- pattern while EuBL onsets was observed (see Section 3, Fig. 4g-i).

We now investigate the 65 ensemble members which capture the observed regime onset in pentad 3. The analysis of the Z500 field shows large positive Z500 anomalies of up to 110 gpm centered over the British Isles (Fig. 5c). These anomalies are very similar to the circulation anomalies around the onset in ERA-Interim (Fig. 2c). The negative anomalies over the western and central North Atlantic are even larger for the Hits compared to ERA-Interim. The results show that the Hits in pentad 3 have very similar circulation anomalies compared to ERA-Interim. In line with the good representation of the Z500 pattern over the North Atlantic and Europe, we find strongly enhanced WCB frequencies over the central North Atlantic for the WCB inflow and centered around Greenland and Iceland for the WCB outflow (Fig. 5a,b). As for Z500, the WCB patterns strongly resemble the 5-day mean frequencies around EuBL onsets in ERA-Interim (Fig. 2a,b). These results indicate a strong link between the correct representation of WCBs and the correct representation of the large-scale circulation in the North Atlantic-European region around EuBL onsets for lead times where the WCB forecast skill has already vanished and the forecast of EuBL becomes increasingly challenging. This finding holds even for the 41 ensemble members with a hit in pentad 4 (Supplement Fig. S1a–c). Thus, local WCB activity in the North Atlantic-European region likely has an impact on the prediction of EuBL onsets and an improved representation of WCBs could provide a pathway to enhanced forecast skill for blocked regimes over Europe even on sub-seasonal time scales.

For observed EuBL onsets in pentad 4, the Misses category does not capture the enhanced WCB activity over the North Atlantic at all (Supplement Fig. S1d,e). The Misses even have negative WCB outflow anomalies (around $-1\,\%$) upstream of the positive geopotential height anomalies. Also in pentad 3 the bulk of ensemble members (1013 of 1078) misses the EuBL onset. We still find slightly enhanced WCB inflow and outflow frequencies (around $1\,\%$) in the Misses category over the North Atlantic (Fig. 5d,e). However, the frequencies are significantly lower than in ERA-Interim or for the Hits category. Further, the amplitude of Z500 anomalies is underestimated and anomalies displaced to the northeast compared to ERA-Interim (Fig. 5f). The results show that the ensemble members that miss EuBL onsets also significantly underestimate WCB frequencies. This further corroborates that WCB activity likely has a strong impact on EuBL predictability and partly explains the low forecast skill of the regime.

4.2 Deciphering cause and effect

So far, we analysed the WCB frequencies in ERA-Interim, the ensemble mean of the reforecast and different subcategories for 5-day mean fields around the onset of EuBL. While this approach gives an overview over the fields around the onset, it does not show if enhanced WCB activity emerges prior to the onset of the regime and directly impacts the development of the block over Europe or if it rather emerges after the onset due to a large-scale circulation that increases cyclone activity over the North Atlantic accompanied by WCB activity upstream of the block. In order to disentangle cause and effect, we calculate lagged frequency composites of WCB activity in ERA-Interim and for the three subcategories of the reforecasts (False Alarms, Hits, and Misses) prior to EuBL onset. We concentrate on results for EuBL onsets in pentad 3, since they are crucial for EuBL life cycles lasting beyond the medium-range and since there is still (some) WCB forecast skill.

The WCB activity in ERA-Interim prior to EuBL onsets is enhanced over eastern Canada and western Europe six to four days before the onset (Fig. 6a). On the other hand, frequencies are below average over the central North Atlantic around Iceland and Greenland. Subsequently, the enhanced outflow activity over eastern Canada shifts eastwards four to two days prior to the EuBL onset (Fig. 6e). Here, WCB frequencies are enhanced from eastern Canada and the southern tip of Greenland to western Europe (anomalies around $5\,\%$). Two to zero days before the EuBL onset, we find a northeastward shift of the main WCB activity with highest frequencies over the northwestern part of Europe and the Norwegian Sea (Fig. 6i). Outflow frequencies are significantly lower than normal over the western North Atlantic. The analysis shows the enhanced WCB outflow frequencies already during the six days before the onset of EuBL. It is therefore very likely that WCB activity contributes to the amplification of the large-scale flow leading to the onset of the blocked regime over Europe.

We now investigate how well the different subcategories of the reforecasts can capture the enhanced WCB frequencies over the North Atlantic prior to EuBL onsets. The False Alarms category has only weak positive WCB outflow frequencies over western Europe six to four days prior to EuBL onsets (Fig. 6b). The outflow anomalies are negative over eastern Canada in a region where frequencies are strongly enhanced in ERA-Interim (Fig. 6a). The Hits category is more similar to ERA-Interim with enhanced frequencies over the western North Atlantic and western Europe (Fig. 6c). However, outflow frequencies over eastern Canada are significantly weaker than in ERA-Interim. In this region, the Misses category captures the enhanced WCB activity better than the Hits with anomalies around 3 % (Fig. 6d). On the other hand, the Misses strongly underestimate WCB outflow frequencies over western Europe.

WCB outflow frequencies increase in the False Alarm category over southern Greenland four to two days before the EuBL onset (Fig. 6f). Similarly, the Hits now exhibit strongly enhanced WCB outflow frequencies over eastern Canada and over southern Greenland (anomalies around 4–6 %) (Fig. 6g). On the other hand, the Misses category shows only weak outflow anomalies in different regions, which are significantly lower compared to the other categories (Fig. 6h). Since the Hits and False Alarms later lead to EuBL, the results corroborate that WCBs over the central North Atlantic four to two days before the onset are an important component in the NWP model to capture the regime onset. If the WCB frequencies are lower, the NWP model struggles to capture the onset of the EuBL regime. Compared to ERA-Interim, Hits and False Alarms have the main WCB outflow farther to the west with significantly lower outflow frequencies over western Europe. This suggests that the NWP model establishes the EuBL regime via WCB activity slightly different than in ERA-Interim.

The last two days before the EuBL onset are characterized by high WCB outflow frequencies (anomalies of 4–6 %) centered over eastern Greenland in the False Alarms category (Fig. 6j). The highest outflow frequencies occur in a similar region for the Hits, while the amplitude of the anomalies is even larger (6–8 %) (Fig. 6k). These findings underline the importance of WCB activity prior to the onset in the ECMWF's IFS reforecasts and corroborate that WCB activity needs to be captured in order to correctly represent blocking over the European region. This is further supported by the Misses category, which lacks enhanced WCB activity completely prior to the onset over the North Atlantic (Fig. 6l) and therefore misses the onset of EuBL and the formation of the corresponding positive Z500 anomaly. It is also noteworthy that the anomalous WCB activity two days prior to EuBL onset differs for False Alarms and Hits in the reforecasts: For False Alarms, WCB outflow is enhanced over the western part of Greenland and Iceland and shifted westward compared to Hits and ERA-interim. Thereby the False Alarms miss the enhanced outflow towards Europe completely. This indicates potential different pathways into the erroneous EuBL for False Alarms and the correct prediction of EuBL in the model.

It is important to note that the results in Fig. 6 are qualitatively very similar for ERA-Interim, as well as the Hits and False Alarms categories when using onsets in pentad 2 or 4 (Supplement Fig. S2 and Fig. S3). However, WCB frequencies are slightly higher for the Misses category for onsets in pentad 2 (Fig. S2d,h,l) and even lower for onsets in pentad 4 (Fig. S3d,h,l). This is in line with the WCB forecast skill, which shows that accurate prediction are still possible in pentad 2 (Fig. 3).

All in all, the lagged analysis of WCB activity before EuBL onsets shows that WCBs are important for the development of the regime. Furthermore, the fact that WCB activity is already enhanced up to 6 days prior to the onset of EuBL corroborates its likely contribution to the establishment of a persistent blocked regime over Europe and is not only a result of an already established circulation that favours WCBs. The findings further underline the potential limitation of EuBL predictions due to the relatively low prediction skill for WCBs and synoptic-scale processes in general. However, they also suggest a potential for increased predictability on sub-seasonal time scales by enhancing the forecast skill of processes governing WCB activity.

5 The role of upstream precursors

We now focus on the role of upstream precursors from the North Pacific for the prediction of EuBL. So far, we revealed concomitant WCB activity over the North Pacific region around EuBL onsets (Fig. 2a,b), which is linked to Rossby wave activity emerging from the western North Pacific (Fig. 2c).

Therefore, we now focus on WCB activity and Z500 fields in ERA-Interim in pentads 1 and 2 prior to EuBL onsets in pentad 3. In pentad 1 enhanced WCB inflow occurs over the western North Pacific (frequencies around 20 %, anomalies around 4 %) and further east over the central North Pacific (anomalies around 4–6 %) (Fig. 7a). In both regions this might be explained by negative Z500 anomalies (Fig. 7c), which likely favour higher cyclone activity and associated WCBs in these regions. Consistent with the WCB inflow, enhanced WCB outflow occurs downstream over the northern part of the central Pacific and further south over the eastern part of the ocean basin (Fig. 7b). Over the North Atlantic WCB activity is weak in pentad 1 and close to climatology.

The anomalously high WCB activity over the North Pacific continues in pentad 2 with positive WCB inflow and outflow anomalies in similar region, as in pentad 1 (Fig. 7d,e). Ongoing WCB outflow in pentad 2 likely contributes to ridge amplification along with positive Z500 anomalies over the eastern Pacific and Alaska, negative Z500 anomalies over western North America, and positive anomalies along the US East Coast (Fig. 7f). This anomaly pattern resembles the anomalous Rossby wave along the midlatitude jet found around the EuBL onset (Fig. 2c). These results highlight that the Rossby wave activity emerges already in pentad 2 before the EuBL onset in pentad 3 and is likely influenced or even triggered by strong WCB activity over the North Pacific. Over the North Atlantic, a negative Z500 anomaly strengthens over Iceland (Fig. 7f) accompanied by increasing WCB outflow to the West in pentad 2 (Fig. 7e). Interestingly, already one pentad prior to EuBL onset a positive Z500 anomaly emerges over northwestern Russia (Fig. 7f) and later persists in that region (cf. Fig. 2c). In summary, strong WCB activity over the North Pacific 5–10 days prior to EuBL onset likely contributes to downstream Rossby wave amplification into the North Atlantic initiating enhanced WCB activity there.

We now evaluate if the found teleconnection affects the ability of IFS reforecasts to predict EuBL onset in pentad 3. Therefore, we first split the ERA-Interim Z500 fields into two subcategories based on Hits and Misses in reforecasts. Note that this weights unique EuBL events according to the ability of the reforecast in predicting the respective EuBL onset. Here, this ability is measured by the number of ensemble members in the Hits and Misses category for each event. If an EuBL event is well predicted (many members in the Hits category), it weights more in the ERA-Interim subcategory based on the Hits and weights less heavily in the subcategory based on the Misses. On the other hand, if an EuBL event is poorly predicted (only few or no members in the Hits category), it is weighted less heavily in the ERA-Interim subcategory based on the Hits and more heavily in the subcategory based on the Misses. The subcategory based on the Hits contains 29 of the 38 unique EuBL events while the subcategory based on the Misses contains all 38 events.

Around EuBL onset in pentad 3, both subcategories show the developing block over Europe with similar positive Z500 anomalies (Fig. 8c,f). Both subcategories also show the concomitant amplified Rossby wave pattern over the North Pacific and North America. However, upstream Z500 anomalies are stronger when reforecasts successfully predict EuBL (Hits) (Fig. 8c). This becomes even more striking in pentads 2 and 1 prior to the EuBL onset in pentad 3 (Fig. 8a,b,d,e). If reforecasts fail in predicting EuBL onset (Misses, Fig. 8d,e), the upstream anomalous Rossby wave activity is almost absent. In contrast marked upstream Rossby wave activity is evident in the subcategory based on Hits with a relatively strong Rossby wave train emerging from the western North Pacific already in pentad 1 (Fig. 8a,b).

These results show that EuBL events with a Rossby wave train emerging from the North Pacific in pentad 1 over the central and eastern North Pacific enable a successful prediction of EuBL onset in ECMWF's IFS reforecasts, while the model struggles in the absence of this teleconnetion. Recalling the link between the Rossby wave train and strong WCB activity over the North Pacific (Fig. 7), inaccurate WCB representation could partly explain the difficulties of the reforecasts in capturing the emerging Rossby wave train and downstream development. We note that the anomalous Rossby wave and WCB activity over the North Pacific might further be related to the Madden-Julian Oscillation (MJO) (Quinting et al., 2023).

Lastly, we directly evaluate the large-scale circulation in IFS reforecasts for the three subcategories Hits, Misses, and False Alarms, in pentads 1 and 2 prior to EuBL onsets in pentad 3. Recall that False Alarms show EuBL onset independent of ERA-Interim. Consistently, the Z500 anomalies for False Alarms shows the trough-ridge couplet typical for EuBL onset in pentad 3 (Fig. 9g), however upstream anomalies are weak and there is no distinct upstream Rossby wave pattern in pentad 1 (Fig. 9a). IFS reforecasts missing EuBL onset in pentad 3 strongly underestimate the developing block over Europe (Fig. 9i) and also feature only weak and indistinct upstream anomalies (Fig. 9c,f). However, successful reforecasts (Hits) not only correctly represent the Z500 anomalies at EuBL onset in pentad 3 (Fig. 9h), they also show a marked concomitant upstream Rossby wave pattern, evident in pentad 2, too, and emerging from the western North Pacific in pentad 1 (Fig. 9b,e). It is noteworthy, that the composites based on reforecast data of successful EuBL onset prediction (Hits, Fig. 9b,e,h) hardly differ from the corresponding Z500 patterns in ERA-Interim (Fig. 8a,b,c). These results corroborate that upstream Rossby wave activity emerging from the western North Pacific 5–10 days prior to EuBL onset provides a potential window of forecast opportunity for EuBL in pentad 3.

6 Conclusions

In this study, we investigated Z500 and WCB activity around the onset of EuBL in ECMWF's IFS sub-seasonal reforecasts and ERA-Interim reanalysis (NDJFM; 1997–2017). EuBL onset is generally not well captured by the reforecasts, which is partly due to its low intrinsic predictability (Faranda et al., 2016; Hochman et al., 2021). Our study newly suggests that for lead times beyond 10 days the model struggles predicting the flow amplification, in particular the ridge building prior to EuBL onset. We find that this is due to a strong link between the Rossby wave amplification around EuBL and enhanced WCB outflow over the central and eastern North Atlantic well before the block establishes. The model misrepresents WCB activity, which ultimately dilutes skill for EuBL forecasts.

For EuBL onsets at early lead times in pentad 2 (5–9 days), the reforecasts can predict the WCB activity and incipient block relatively well. This is in line with the overall WCB forecast skill, which is still sufficient on these time scales (Wandel et al., 2021). However, onsets in pentad 3 (10–14 days) and pentad 4 (15–19 days) are challenging for the NWP model. The model strongly underestimates WCB activity and subsequently the developing block prior to onsets in pentad 3 and on average misses onsets in pentad 4 completely.

Time-lagged analysis reveals that the enhanced WCB activity emerges from the western North Atlantic already six days prior to EuBL onset - well before any indication of blocking over Europe. In addition stratification of the reforecasts according to Hits, Misses, and False Alarms of EuBL onset in pentad 3 and pentad 4 shows different pathways towards EuBL onset. For successful predictions of EuBL onset (Hits), the model accurately represents the enhanced WCB activity prior to EuBL onset, whereas for Misses it completely misses WCB activity. Thus, a correct representation of WCB activity provides a potential window of forecast opportunity for EuBL forecasts beyond 10 days. In contrast for False Alarms, enhanced WCB activity only emerges directly (-2 to 0 days) prior to blocking onset and WCB outflow occurs farther to the west over eastern Greenland and Iceland missing enhanced WCB outflow over Europe which is evident in ERA-Interim and the Hits forecasts. This shows that the model has an additional erroneous pathway into EuBL.

We further find a potential teleconnection to the North Pacific region. Enhanced WCB activity emerges from the western North Pacific region up to 10 days prior to EuBL onset and goes along with downstream development of an amplified Rossby wave pattern (Grams & Archambault, 2016; Röthlisberger et al., 2018). Rossby wave activity propagates downstream over North America into the North Atlantic region initiating WCB activity there. These upstream precursors are remarkably similar in ERA-Interim and successful reforecasts (Hits) but missing for erroneous EuBL forecasts (False Alarms) and Misses.

Thus, forecast errors related to strong WCB activity over the North Pacific could dilute the Rossby wave signal and subsequently lead to errors in the downstream flow patterns and the prediction of EuBL onsets. On the other hand, the teleconnection from the North Pacific region provides another window of forecast opportunity for the prediction of EuBL onset into sub-seasonal timescales and likely depends on an accurate representation of WCB activity conditioned on the MJO in the North Pacific region, too (Quinting et al., 2023).

In summary, our results highlight the role of moist dynamical processes for the correct prediction of EuBL onset. On the one hand, a correct representation of WCB activity in the North Atlantic region in the days prior to EuBL onset results in correct EuBL forecasts. On the other hand, a correct representation of the teleconnection established via Rossby wave activity emerging from the North Pacific extends correct EuBL forecasts into sub-seasonal lead times. Interestingly the North Pacific Rossby wave pattern is also amplified by WCB activity, in line with recent findings by Quinting et al. (2023) who highlight the potential role of WCBs in shaping tropical-extratropical teleconnection patterns due to MJO. If and how the MJO further affects EuBL onset should be a subject of future work. Our results further suggest, that improving the representation of WCB activity in numerical models likely yields a better representations of EuBL life cycles, too. The improvement of WCB activity is linked to a more accurate depiction of extratropical cyclones, offering the potential to increase forecast skill, even for sub-seasonal lead times.

7 Open Research

ECMWF's sub-seasonal reforecasts from 1997–2017 are freely available at `https://apps.ecmwf.int/datasets/data/s2s/` and ERA-Interim data are freely available at `https://apps.ecmwf.int/datasets/data/interim-full-daily/`. Code for the CNN method is provided via the repository at `https://git.scc.kit.edu/nk2448/wcbmetric_v2.git`.

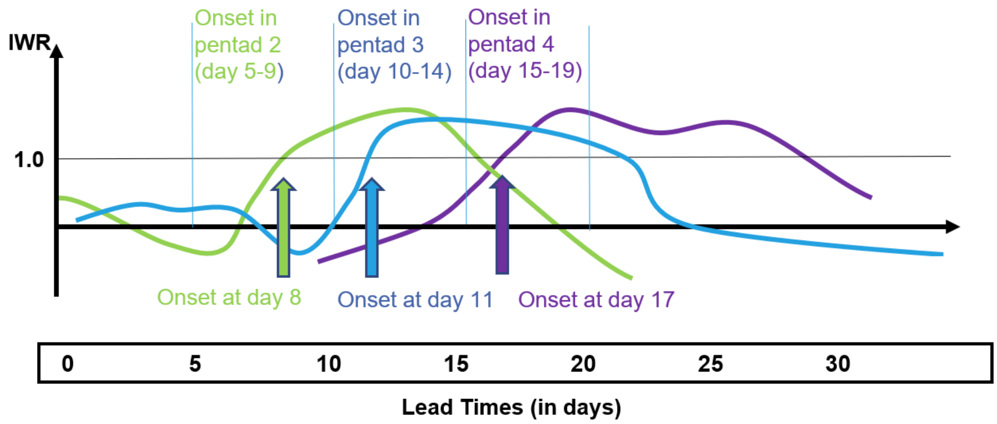

Figure 1. Schematic of weather regime life cycle based on weather regime index I_{wr}. The onset is defined as the day when I_{wr} exceeds a certain threshold. Here, regime onsets in pentad 2 (day 5–9), pentad 3 (day 10–14) and pentad 4 are investigated. They can occur at any day in a given pentad.

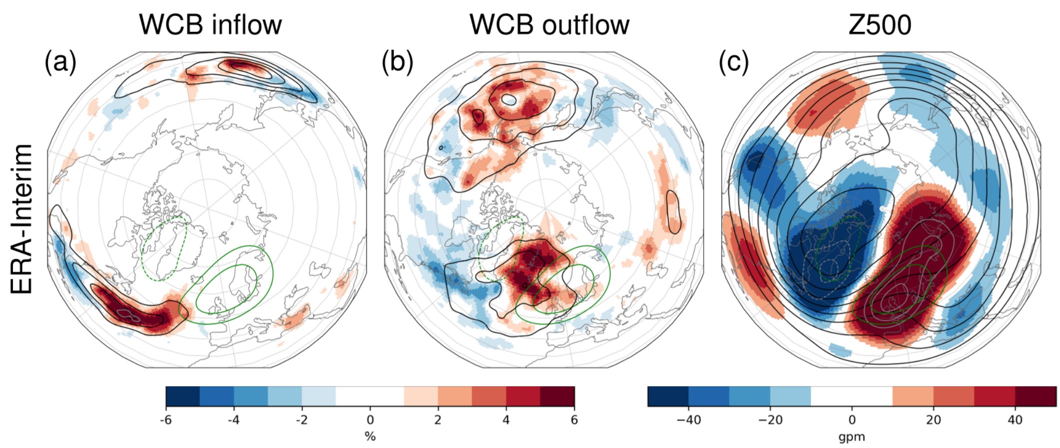

Figure 2. WCB inflow (a), WCB outflow (b), and 500 hPa geopotential height anomalies (c) anomalies (shading) around EuBL onsets in ERA-Interim (5-day mean in pentad 3; NDJFM, 1997–2017; ERA-Interim treated as the "perfect ensemble member"). Black contours indicate absolute fields (frequencies ranging from 5-20% every 5% in (a) and (b), and 5100–5800 gpm, every 100 gpm in (c)). Grey contours highlight anomalies exceeding the color bar (6 %,8 % in (a) and (b), and –90,–70,70,90,110 gpm in (c)). Green contours indicate geopotential height anomalies (–50,50,100 gpm) for all ERA-Interim EuBL cases from 1979–2015.

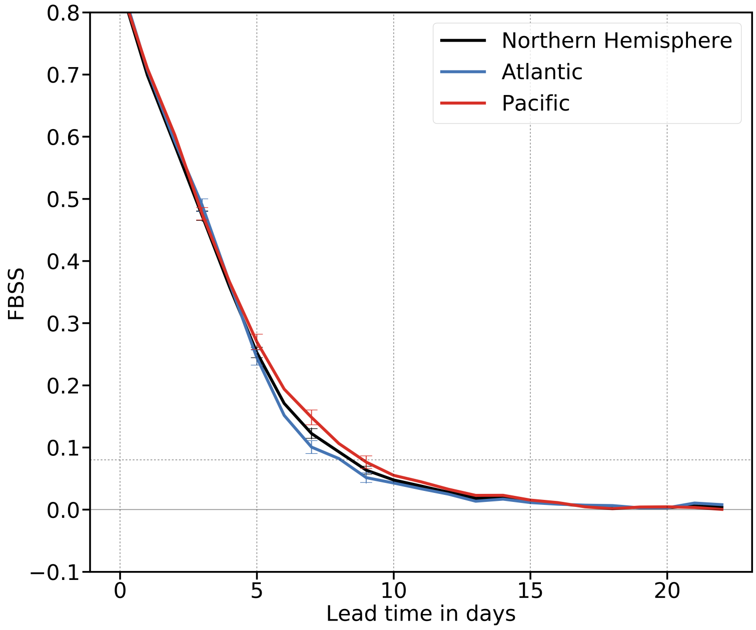

Figure 3. Area-averaged Fair Brier Skill Score ($FBSS$) for DJF 1997–2017 at different forecast lead times for WCB outflow. The area-average of the $FBSS$ is computed over the North Atlantic (20–90 , 100 W–20 E), North Pacific (20–90 N, 120 E–120 W) and for the entire Northern Hemisphere. Error bars centered on forecast lead times day 3, 5, 7, and 9 show the difference between the 10 and 90 th percentile of the sampled data (variability of the $FBSS$) and are used to estimate the significant differences between the ocean basins.

Table 1. Number of EuBL events in NDJFM (1997–2017) for ERA-Interim and different categories of the ECMWF's IFS reforecasts (Hits, Misses, False Alarms; see Section 2.4 for explanation)

Hits	Unique events	Forecast perspective	Ensemble members
Pentad 2	34	72	271
Pentad 3	29	45	65
Pentad 4	26	34	41
Misses	Unique events	Forecast perspective	Ensemble members
Pentad 2	38	97	807
Pentad 3	38	98	1013
Pentad 4	38	98	1037
False Alarms		Forecast Perspective	Ensemble members
Pentad 2		362	728
Pentad 3		540	808
Pentad 4		644	848

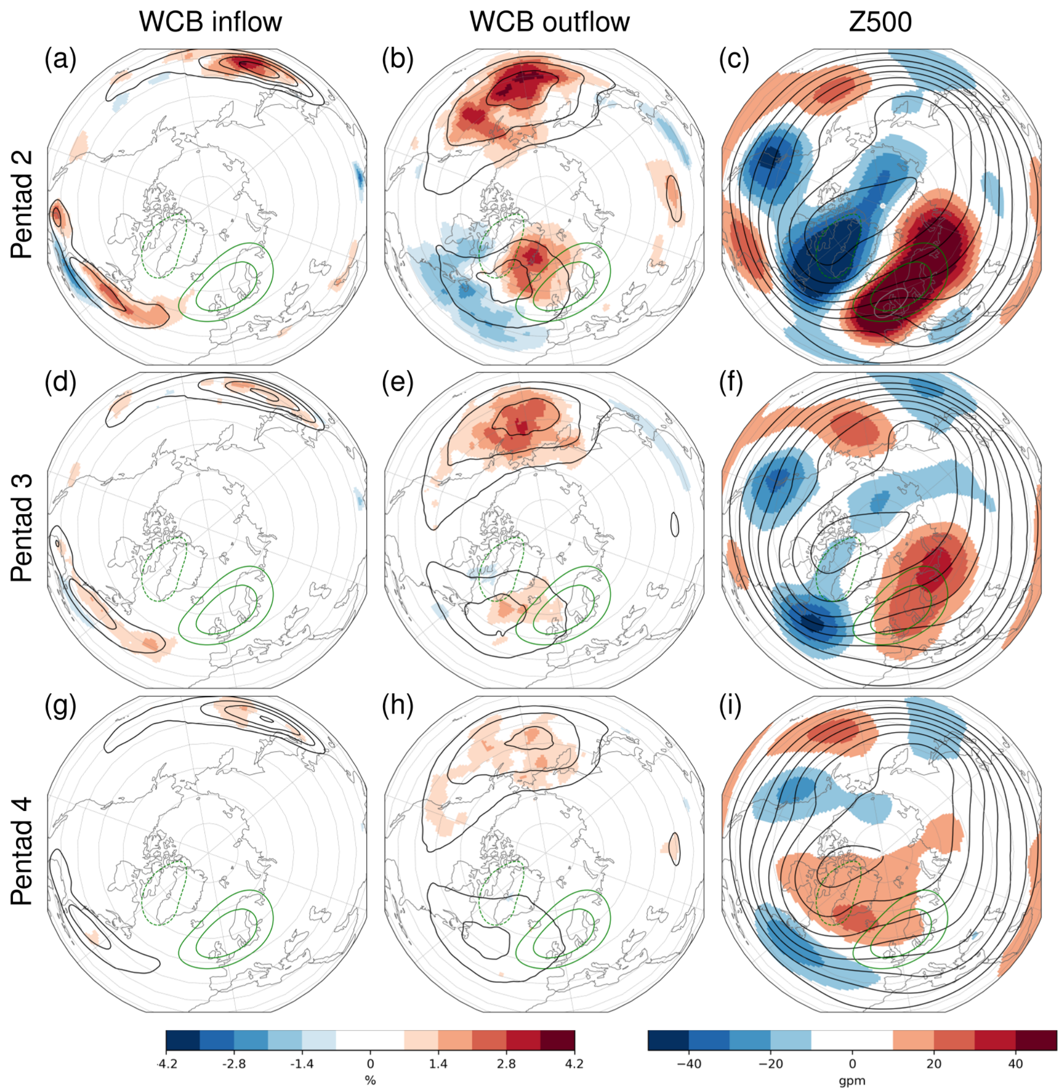

Figure 4. Ensemble mean prediction (ECMWF's IFS reforecasts; NDJFM 1997–2017) of EuBL onsets in ERA-Interim in (a-c) pentad 2, (d-f) pentad 3, and (g-i) pentad 4. Plots show 5-day mean anomalies (shading) of ensemble mean forecasts in different pentads for (a,d,g) WCB inflow, (b,e,h) WCB outflow and (c,f,i) Z500, as well as 5-day mean WCB frequencies (black contours; 5,10,15,20 % in (a,b,d,e,g,h) and Z500 fields (black contours; 5100–5800 gpm, every 100 gpm in (c,f,i)). Green contours as in Fig. 2.

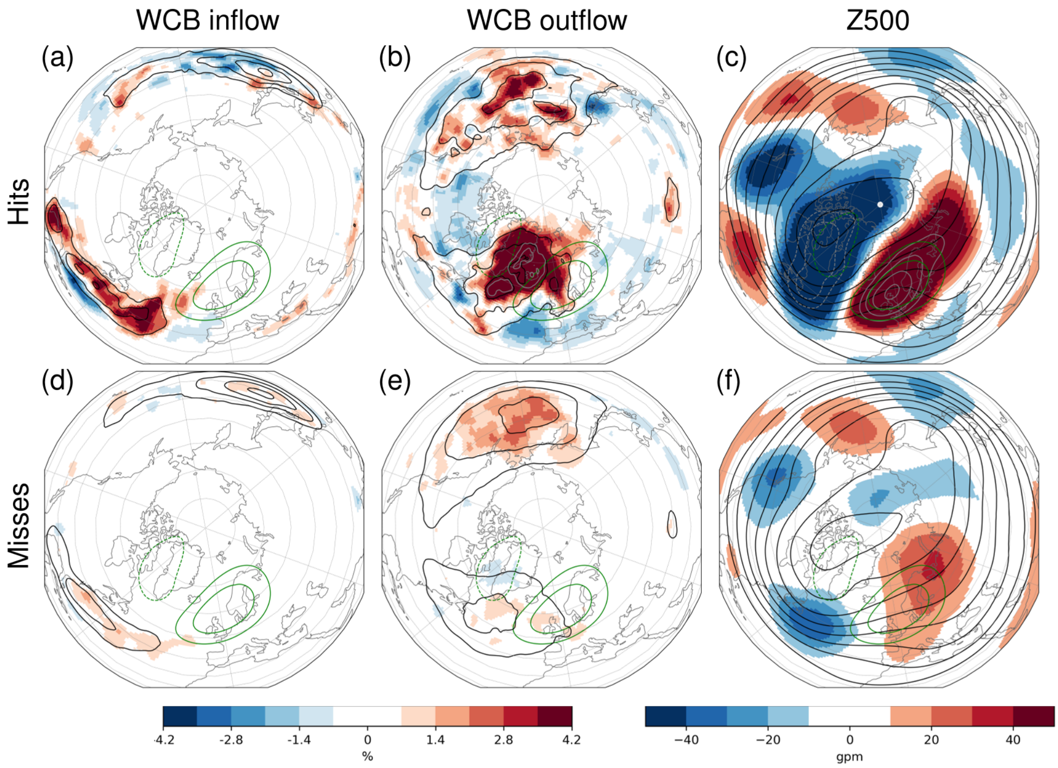

Figure 5. (a–c) Ensemble members with a correct representation of ERA-Interim EuBL onset (Hits) and (d–f) ensemble members missing ERA-interim onsets (Misses) in pentad 3 (5-day mean of (a,d) WCB inflow, (b,e) WCB outflow and (c,f) Z500 anomalies (shading) and absolute frequencies (contours) as in Fig. 4 (ECMWF's IFS reforecasts, NDJFM, 1997–2017)). Grey contours show strong WCB anomalies (6, 8 %) and Z500 anomalies (–90,70,90,110,130 gpm). Green contours as in Fig. 2.

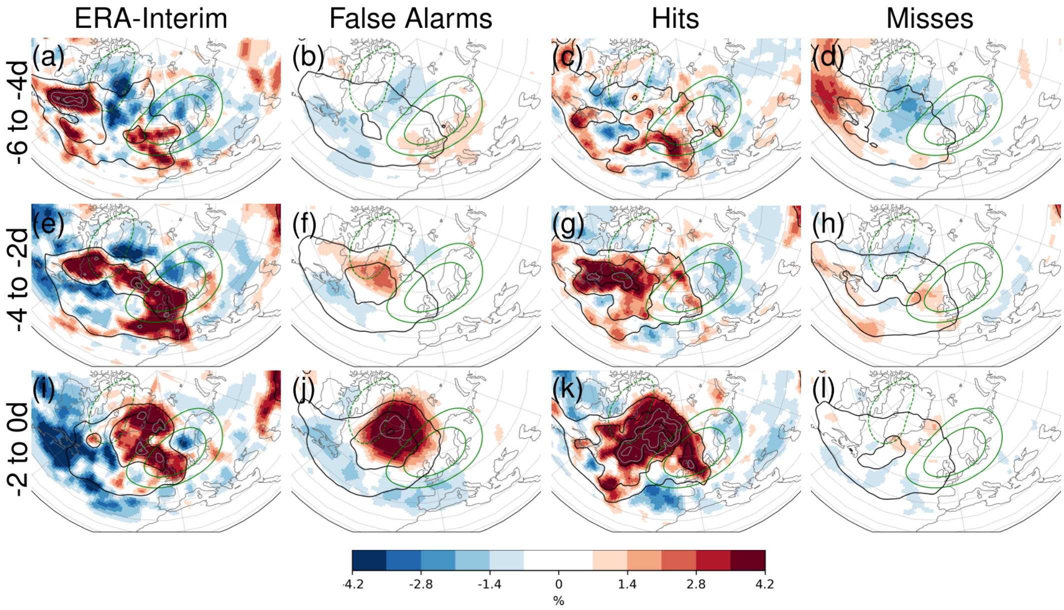

Figure 6. WCB outflow frequency anomalies (shading) 6 to 4 days (a-d), 4 to 2 days (e–h), and 2 to 0 days (i–l) prior to EuBL onset in pentad 3 in a),e),i) ERA-Interim (NDJFM; 1997–2017), b),f),j) False Alarms, c),g),k) Hits, d),h),l) Misses (ECMWF's IFS reforecasts; NDJFM, 1997–2017). Grey contours show strong WCB outflow anomalies (6,8,10 %) and black contours indicate absolute WCB outflow (5,10,15,20 %). Green contours as in Fig. 2.

Acknowledgments

This research was funded by the Helmholtz Association as part of the Young Investigator Group "Sub-seasonal Predictability: Understanding the Role of Diabatic Outflow" (SPREADOUT, grant VH-NG-1243) and was partially embedded in the subprojects A8 and B8 of the Transregional Collaborative Research Center SFB/TRR 165 "Waves to Weather" (`https://www.wavestoweather.de`) funded by the German Research Foundation (DFG). The work is based on S2S data. S2S is a joint initiative of the World Weather Research Programme (WWRP) and the World Climate Research Programme (WCRP). The original S2S database is hosted at ECMWF as an extension of the TIGGE database. We thank thank the large-scale dynamics and predictability group at KIT namely Moritz Pickl, Seraphine Hauser, Joshua Dorrington, Fabian Mockert, Annika Oertel, Marisol Osman, and Marta Wenta for many fruitful discussions and ideas for the manuscript. Furthermore, we thank colleagues from ECMWF (Magdalena Alonso Balmaseda, Linus Magnusson, Frédéric Vitart, and Chris Roberts) for their comments on our results. Lastly, we acknowledge the ECMWF and Deutscher Wetterdienst for granting access to the ERA-Interim dataset.

References

Anstey, J. A., Davini, P., Gray, L. J., Woollings, T. J., Butchart, N., Cagnazzo, C., ... Yang, S. (2013). Multi-model analysis of Northern Hemisphere winter blocking: Model biases and the role of resolution. *Journal of Geophysical Research: Atmospheres*, *118*(10), 3956–3971.

Berggren, R., Bolin, B., & Rossby, C.-G. (1949). An aerological study of zonal motion, its perturbations and break-down. *Tellus*, *1*(2), 14–37.

Berman, J. D., & Torn, R. D. (2019). The impact of initial condition and warm

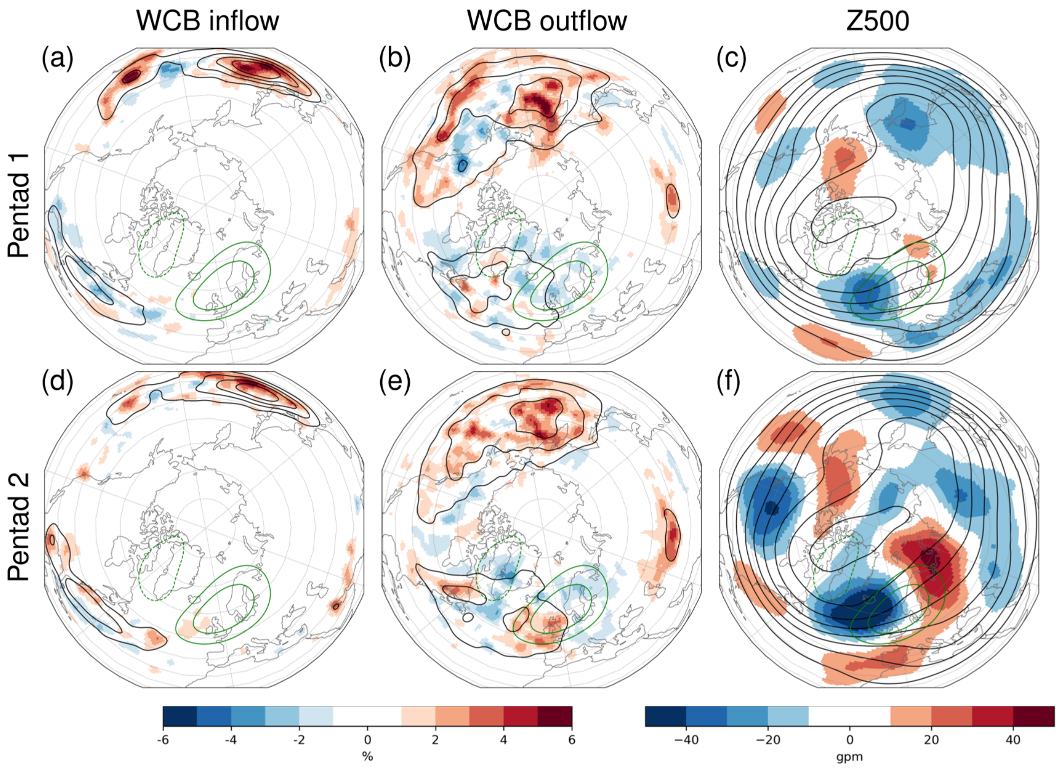

Figure 7. Evolution of 5-day mean (a,d) WCB inflow, (b,e) WCB outflow and (c,f) Z500 in ERA-Interim in (a–c) pentad 1 and (d-f) pentad 2 before ERA-Interim EuBL onsets in pentad 3 (ERA-Interim treated as the "perfect ensemble member"). WCB and Z500 anomalies (shading), absolute fields (contours) and green contours as in Fig. 2.

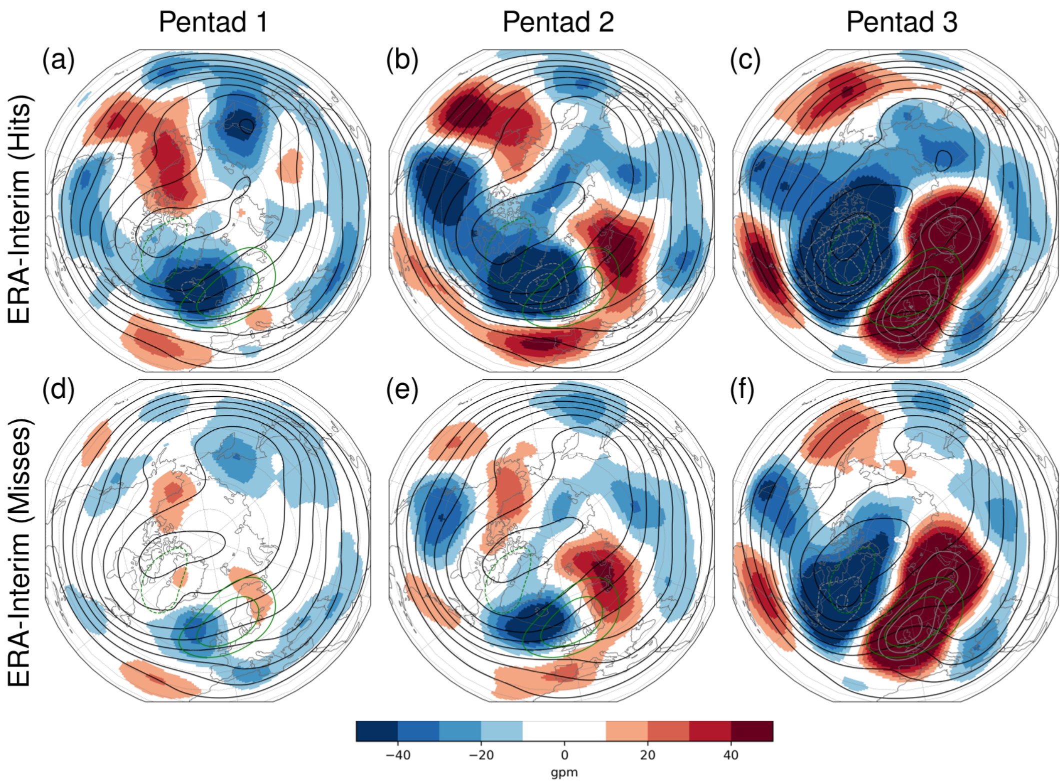

Figure 8. Evolution of 5-day mean Z500 in ERA-Interim weighted with the amount of (a–c) Hits (29 unique events, see Tab. 1) and (d–e) Misses (38 unique events) for each respective forecast intitial time in (a,d) pentad 1 and (b,d) pentad 2 before ERA-Interim EuBL onsets in (c,f) pentad 3. Z500 anomalies (shading), absolute fields (contours) and green contours as in Fig. 2.

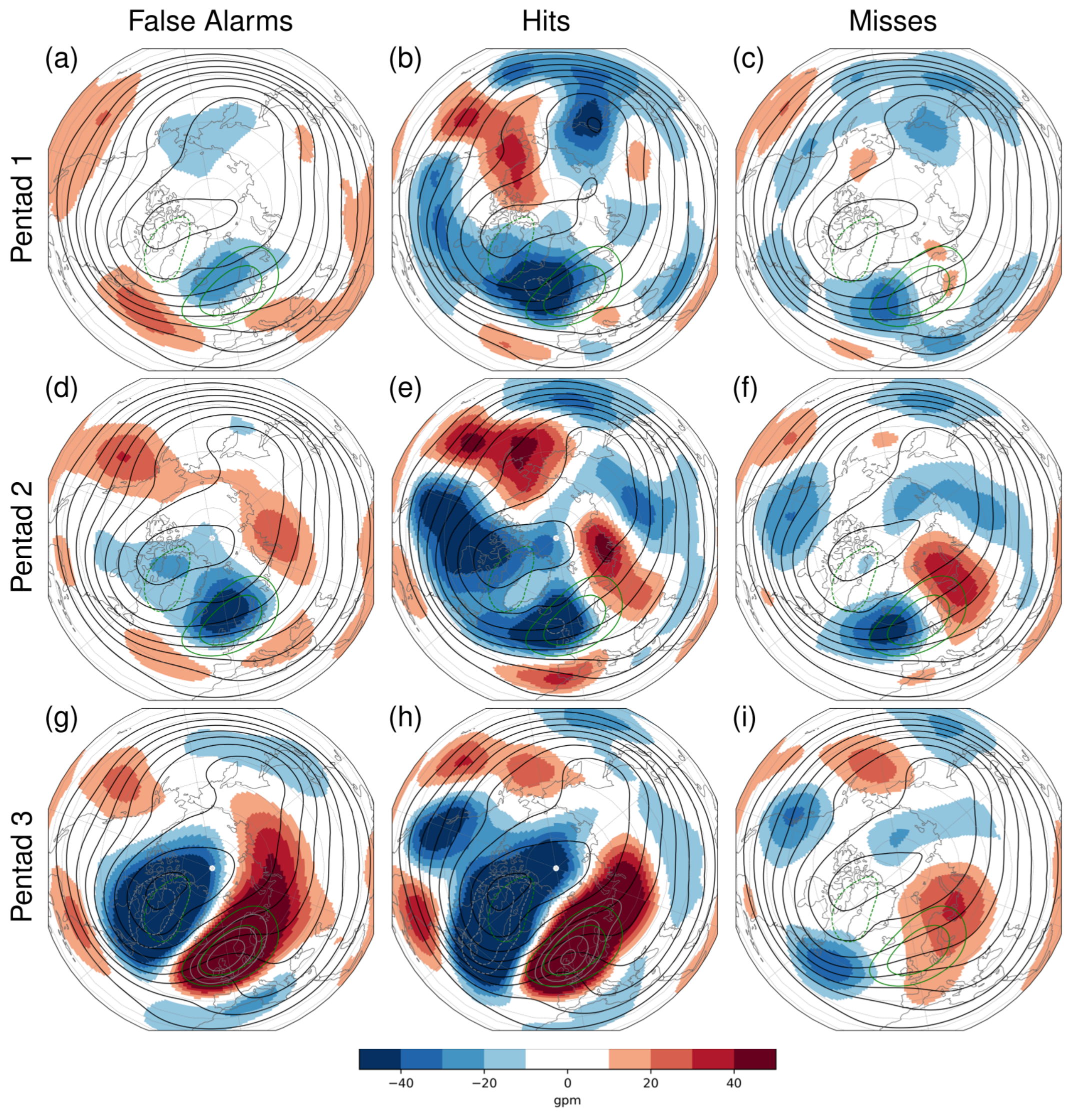

Figure 9. Evolution of 5-day mean Z500 anomalies (shading) for (a,d,g) False Alarms, (b,e,h) Hits, and (c,f,i) Misses (ECMWF's IFS reforecasts, NDJFM, 1997–2017) in (a–c) pentad 1, (d–f) pentad 2, and (g–i) pentad 3 prior to and around EuBL onsets in pentad 3. Grey contours show strong Z500 anomalies (–90,–70,70,90,110,130 gpm) and black contours indicate absolute Z500 fields (5100–5800 gpm, every 100 gpm). Green contours as in Fig. 2.

conveyor belt forecast uncertainty on variability in the downstream waveguide in an ecwmf case study. *Monthly Weather Review*, *147*(11), 4071–4089.
Bloomfield, H. C., Brayshaw, D. J., Gonzalez, P. L., & Charlton-Perez, A. (2021). Pattern-based conditioning enhances sub-seasonal prediction skill of european national energy variables. *Meteorological Applications*, *28*(4), e2018.
Buehler, T., Raible, C. C., & Stocker, T. F. (2011). The relationship of winter season North Atlantic blocking frequencies to extreme cold or dry spells in the ERA-40. *Tellus A: Dynamic Meteorology and Oceanography*, *63*(2), 174–187.
Büeler, D., Ferranti, L., Magnusson, L., Quinting, J. F., & Grams, C. M. (2021). Year-round sub-seasonal forecast skill for Atlantic-European weather regimes. *Quarterly Journal of the Royal Meteorological Society*.
Charney, J. G., & DeVore, J. G. (1979). Multiple flow equilibria in the atmosphere and blocking. *Journal of Atmospheric Sciences*, *36*(7), 1205–1216.
Colucci, S. J. (1985). Explosive cyclogenesis and large-scale circulation changes: Implications for atmospheric blocking. *Journal of Atmospheric Sciences*, *42*(24), 2701–2717.
Davini, P., Corti, S., D'Andrea, F., Rivière, G., & von Hardenberg, J. (2017). Improved winter European atmospheric blocking frequencies in high-resolution global climate simulations. *Journal of Advances in Modeling Earth Systems*, *9*(7), 2615–2634.
Dawson, A., Palmer, T., & Corti, S. (2012). Simulating regime structures in weather and climate prediction models. *Geophysical Research Letters*, *39*(21).
Dee, D. P., Uppala, S. M., Simmons, A., Berrisford, P., Poli, P., Kobayashi, S., … others (2011). The ERA-Interim reanalysis: Configuration and performance of the data assimilation system. *Quarterly Journal of the royal meteorological society*, *137*(656), 553–597.
Dole, R. M. (1986). The life cycles of persistent anomalies and blocking over the North Pacific. In *Advances in geophysics* (Vol. 29, pp. 31–69). Elsevier.
d'Andrea, F., Tibaldi, S., Blackburn, M., Boer, G., Déqué, M., Dix, M., … others (1998). Northern Hemisphere atmospheric blocking as simulated by 15 atmospheric general circulation models in the period 1979–1988. *Climate Dynamics*, *14*(6), 385–407.
Faranda, D., Masato, G., Moloney, N., Sato, Y., Daviaud, F., Dubrulle, B., & Yiou, P. (2016). The switching between zonal and blocked mid-latitude atmospheric circulation: a dynamical system perspective. *Climate Dynamics*, *47*(5), 1587–1599.
Ferranti, L., Corti, S., & Janousek, M. (2015). Flow-dependent verification of the ECMWF ensemble over the Euro-Atlantic sector. *Quarterly Journal of the Royal Meteorological Society*, *141*(688), 916–924.
Ferranti, L., Magnusson, L., Vitart, F., & Richardson, D. S. (2018). How far in advance can we predict changes in large-scale flow leading to severe cold conditions over Europe? *Quarterly Journal of the Royal Meteorological Society*, *144*(715), 1788–1802.
Ferro, C. (2014). Fair scores for ensemble forecasts. *Quarterly Journal of the Royal Meteorological Society*, *140*(683), 1917–1923.
Grams, C. M., & Archambault, H. M. (2016). The key role of diabatic outflow in amplifying the midlatitude flow: A representative case study of weather systems surrounding western North Pacific extratropical transition. *Monthly Weather Review*, *144*(10), 3847–3869.
Grams, C. M., Beerli, R., Pfenninger, S., Staffell, I., & Wernli, H. (2017). Balancing Europe's wind-power output through spatial deployment informed by weather regimes. *Nature climate change*, *7*(8), 557–562.
Grams, C. M., Magnusson, L., & Madonna, E. (2018). An atmospheric dynamics perspective on the amplification and propagation of forecast error in numerical weather prediction models: A case study. *Quarterly Journal of the Royal*

Meteorological Society, *144* (717), 2577–2591.

Grams, C. M., Wernli, H., Böttcher, M., Čampa, J., Corsmeier, U., Jones, S. C., . . . Wiegand, L. (2011). The key role of diabatic processes in modifying the upper-tropospheric wave guide: a North Atlantic case-study. *Quarterly Journal of the Royal Meteorological Society*, *137* (661), 2174–2193.

Hochman, A., Messori, G., Quinting, J. F., Pinto, J. G., & Grams, C. M. (2021). Do Atlantic-European weather regimes physically exist? *Geophysical Research Letters*, e2021GL095574.

Hoskins, B. J., & Karoly, D. J. (1981). The steady linear response of a spherical atmosphere to thermal and orographic forcing. *Journal of Atmospheric Sciences*, *38* (6), 1179–1196.

Jia, X., Yang, S., Song, W., & He, B. (2014). Prediction of wintertime northern hemisphere blocking by the NCEP climate forecast system. *Journal of meteorological research*, *28* (1), 76–90.

Madonna, E., Wernli, H., Joos, H., & Martius, O. (2014). Warm conveyor belts in the ERA-Interim dataset (1979–2010). Part I: Climatology and potential vorticity evolution. *Journal of Climate*, *27* (1), 3–26.

Martínez-Alvarado, O., Madonna, E., Gray, S. L., & Joos, H. (2016). A route to systematic error in forecasts of rossby waves. *Quarterly Journal of the Royal Meteorological Society*, *142* (694), 196–210.

Masato, G., Woollings, T., & Hoskins, B. (2014). Structure and impact of atmospheric blocking over the Euro-Atlantic region in present-day and future simulations. *Geophysical Research Letters*, *41* (3), 1051–1058.

Mastrantonas, N., Magnusson, L., Pappenberger, F., & Matschullat, J. (2022). What do large-scale patterns teach us about extreme precipitation over the mediterranean at medium-and extended-range forecasts? *Quarterly Journal of the Royal Meteorological Society*, *148* (743), 875–890.

Michel, C., & Rivière, G. (2011). The link between Rossby wave breakings and weather regime transitions. *Journal of the Atmospheric Sciences*, *68* (8), 1730–1748.

Michel, C., Rivière, G., Terray, L., & Joly, B. (2012). The dynamical link between surface cyclones, upper-tropospheric Rossby wave breaking and the life cycle of the Scandinavian blocking. *Geophysical Research Letters*, *39* (10). doi: 10.1029/2012GL051682

Michelangeli, P.-A., Vautard, R., & Legras, B. (1995). Weather regimes: Recurrence and quasi stationarity. *Journal of the atmospheric sciences*, *52* (8), 1237–1256.

Mohr, S., Wandel, J., Lenggenhager, S., & Martius, O. (2019). Relationship between atmospheric blocking and warm-season thunderstorms over western and central Europe. *Quarterly Journal of the Royal Meteorological Society*, *145* (724), 3040–3056.

Nakamura, N., & Huang, C. S. (2018). Atmospheric blocking as a traffic jam in the jet stream. *Science*, *361* (6397), 42–47.

Osman, M., Beerli, R., Büeler, D., & Grams, C. M. (2023). Multi-model Assessment of Sub-seasonal Predictive Skill for Year-round Atlantic-European Weather Regimes. *Quarterly Journal of the Royal Meteorological Society*, *n/a*(n/a). doi: 10.1002/qj.4512

Pfahl, S., Schwierz, C., Croci-Maspoli, M., Grams, C. M., & Wernli, H. (2015). Importance of latent heat release in ascending air streams for atmospheric blocking. *Nature Geoscience*, *8* (8), 610–614.

Pfahl, S., & Wernli, H. (2012). Quantifying the relevance of atmospheric blocking for co-located temperature extremes in the Northern Hemisphere on (sub-) daily time scales. *Geophysical Research Letters*, *39* (12).

Pickl, M., Quinting, J. F., & Grams, C. M. (2023). Warm conveyor belts as amplifiers of forecast uncertainty. *Quarterly Journal of the Royal Meteorological Society*.

Pomroy, H. R., & Thorpe, A. J. (2000). The evolution and dynamical role of reduced upper-tropospheric potential vorticity in intensive observing period one of FASTEX. *Monthly Weather Review*, *128*(6), 1817–1834.

Quinting, J., & Grams, C. (2022). Eulerian Identification of ascending AirStreams (ELIAS 2.0) in numerical weather prediction and climate models. Part I: Development of deep learning model. *Geoscientific Model Development*, *15*, 715–730.

Quinting, J., Grams, C. M., Chang, E. K.-M., Pfahl, S., & Wernli, H. (2023). Warm conveyor belt activity over the pacific: Modulation by the madden-julian oscillation and impact on tropical-extratropical teleconnections. *EGUsphere*, *2023*, 1–31.

Quinting, J., & Vitart, F. (2019). Representation of synoptic-scale Rossby wave packets and blocking in the S2S prediction project database. *Geophysical Research Letters*, *46*(2), 1070–1078.

Rex, D. F. (1950). Blocking action in the middle troposphere and its effect upon regional climate. *Tellus*, *2*(4), 275–301.

Rodwell, M. J., Magnusson, L., Bauer, P., Bechtold, P., Bonavita, M., Cardinali, C., ... others (2013). Characteristics of occasional poor medium-range weather forecasts for Europe. *Bulletin of the American Meteorological Society*, *94*(9), 1393–1405.

Röthlisberger, M., Martius, O., & Wernli, H. (2018). Northern Hemisphere Rossby wave initiation events on the extratropical jet—A climatological analysis. *Journal of Climate*, *31*(2), 743–760.

Shutts, G. (1983). The propagation of eddies in diffluent jetstreams: Eddy vorticity forcing of 'blocking'flow fields. *Quarterly Journal of the Royal Meteorological Society*, *109*(462), 737–761.

Steinfeld, D., & Pfahl, S. (2019). The role of latent heating in atmospheric blocking dynamics: a global climatology. *Climate Dynamics*, *53*(9), 6159–6180.

Vautard, R. (1990). Multiple weather regimes over the North Atlantic: Analysis of precursors and successors. *Monthly weather review*, *118*(10), 2056–2081.

Vitart, F. (2017). Madden—Julian Oscillation prediction and teleconnections in the S2S database. *Quarterly Journal of the Royal Meteorological Society*, *143*(706), 2210–2220.

Wandel, J., Quinting, J. F., & Grams, C. M. (2021). Toward a systematic evaluation of warm conveyor belts in numerical weather prediction and climate models. Part II: Verification of operational reforecasts. *Journal of the Atmospheric Sciences*, *78*(12), 3965–3982.

Wernli, H. (1997). A Lagrangian-based analysis of extratropical cyclones. II: A detailed case-study. *Quarterly Journal of the Royal Meteorological Society*, *123*(542), 1677–1706.

Wernli, H., & Davies, H. C. (1997). A Lagrangian-based analysis of extratropical cyclones. I: The method and some applications. *Quarterly Journal of the Royal Meteorological Society*, *123*(538), 467–489.

Yamazaki, A., & Itoh, H. (2013). Vortex–vortex interactions for the maintenance of blocking. Part I: The selective absorption mechanism and a case study. *Journal of the atmospheric sciences*, *70*(3), 725–742.